Available online at www.sciencedirect.com
SCIENCE DIRECT®
Journal of Solid State Chemistry 177 (2004) 3748–3751
JOURNAL OF SOLID STATE CHEMISTRY
www.elsevier.com/locate/jssc

New transparent conductors with the M_7O_{12} ordered oxygen-deficient fluorite structure: from $In_4Sn_3O_{12}$ to $In_{5.5}Sb_{1.5}O_{12}$

J. Choisnet*, L. Bizo, R. Retoux, S. Hébert, B. Raveau

Laboratoire de cristallographie et sciences des materiaux (CRISMAT), UMR 6508 CNRS-ISMRA, 6 Boulevard du Maréchal Juin, 14050 Caen, Cédex, France

Received 29 June 2004; accepted 13 July 2004
Available online 27 August 2004

Abstract

A new transparent conductor, containing pentavalent antimony, $In_{4+x}Sn_{3-2x}Sb_xO_{12}$, has been synthesized for $0 \leqslant x \leqslant 1.5$. The latter exhibits an ordered oxygen-deficient fluorite structure with an ordered distribution of Sb^{5+} and In^{3+}/Sn^{4+} species in the octahedral and seven-fold coordinated sites, respectively. More importantly, it is shown that the electronic conductivity of this transparent conducting oxide (TCO) at room temperature, is one order of magnitude larger for $x = 1$ (In_5SnSbO_{12}) than for $x = 0$ ($In_4Sn_3O_{12}$) and it turns to a semi-metallic behavior in contrast to $In_4Sn_3O_{12}$ which is a semi-conductor. The potential of this new material, as TCO, is also shown by its reflectance spectra, similar to $In_4Sn_3O_{12}$, involving only a small increase of the optical bandgap, by 0.15 eV.
© 2004 Elsevier Inc. All rights reserved.

Keywords: Indium tin antimonates; Transparent conductors; Oxygen-deficient fluorite type; Indium-antimony ordering

The importance of transparent conducting oxides (TCO) in the field of optoelectronics for various devices such as solar cells, electroluminescence and liquid crystal displays [1], has been extended dramatically these recent years with the event of flat screen high-definition televisions, high-resolution screens of portable computers, thin film photovoltaïcs and electrochromic windows [2–3]. For these reasons, numerous investigations have been carried out recently on these materials, in order to discover new *n*-type [4–5] or *p*-type [6] transparent conductors. Among the various *n*-type TCOs that have been found up to now, the indium tin doped oxide In_2O_3:Sn, known as ITO, appears as most famous [7–11]. Besides this indium-rich oxide, which crystallizes with the bixbyite structure, another oxide was identified for the composition $In_4Sn_3O_{12}$ [12–14]. Thin films of the latter oxides were found to be highly conducting and transparent [15], with characteristics close to ITO. The structural study of this M_7O_{12} oxide [16] showed that its rhombohedral structure is closely related to the bixbyite type, and is in fact a doubly ordered oxygen-deficient fluorite, on both cationic and anionic sites.

Bearing in mind that in such a In–Sn–O system the In^{3+} and Sn^{4+} cations both exhibit a d^{10} electronic outer configuration, we have investigated the possible substitution of the pair antimony (V)–indium(III) for tin (IV). In the present paper, we show the great ability of Sb(V) to form the M_7O_{12} ordered oxygen-deficient fluorite structure and demonstrate that the ordering phenomena hold for the whole solid solution $In_{4+x}Sn_{3-2x}Sb_xO_{12}$ ($0 \leqslant x \leqslant 1.5$). More importantly, we show that the introduction of antimony increases the electronic conductivity up to one order of magnitude with respect to $In_4Sn_3O_{12}$ [15], leading to a practically semi-metallic behavior for In_5SnSbO_{12}, in contrast to $In_4Sn_3O_{12}$ which is a semi-conductor. The potential of these Sb phases as transparent conductors is also shown by their reflectance spectra, similar to that of $In_4Sn_3O_{12}$.

*Corresponding author. Fax: +33-2-31-95-16-00.
E-mail address: jacques.choisnet@ismra.fr (J. Choisnet).

0022-4596/$ - see front matter © 2004 Elsevier Inc. All rights reserved.
doi:10.1016/j.jssc.2004.07.039

Six compositions ($x = 0.33$; 0.50; 0.66; 1; 1.33; 1.50) of the solid solution $In_{4+x}Sn_{3-2x}Sb_xO_{12}$ and $In_4Sn_3O_{12}$ for comparison, were prepared from mixtures of pure In_2O_3, SnO_2 and Sb_2O_3 powder oxides, in alumina crucibles heated in air. After an initial heating at 600 °C in order to ensure the full oxidation of Sb(III) into Sb(V), successive 12 h annealings followed by air quenching, were performed at increasing temperatures up to 1400 °C, except for the richest Sb compositions ($x = 1.33$; 1.50), which were heated up to 1250 °C, in order to prevent any decomposition. It was checked that no supplementary weight loss due to the presence of antimony, occurred during the whole series of annealings. According to this experimental procedure, pure phases corresponding to the entire range of solid solution $In_{4+x}Sn_{3-2x}Sb_xO_{12}$ ($0 \leqslant x \leqslant 1.5$) were isolated. The X-ray powder diffraction (XRPD) patterns of these phases are isotypic to $In_4Sn_3O_{12}$, as shown for the limit antimony indate $In_{5.5}Sb_{1.5}O_{12}$ (Fig. 1). The ability of formation of the M_7O_{12} type phases is undoubtly favored by a progressive introduction of antimony. Energy dispersive spectroscopy using a Kevex analyzer mounted on a Jeol 200CX electron microscope, was carried out on more than 50 microcrystals. It confirms the great homogeneity of the samples. The presence of any other element than In, Sn and Sb was never detected. The observed cationic composition agrees with the nominal one. Moreover, the cationic distribution does not fluctuate significantly from one microcrystallite to the other, for a given sample.

XRPD structure calculations were performed from a Rietveld analysis (Fullprof program [17]) of the diffractograms recorded on a Philips vertical goniometer (Cu$K\alpha$ radiation), equipped with a secondary graphite monochromator, in the angular range 6–120°, 2θ. The structural model of $In_4Sn_3O_{12}$ [16] was used: S.G. $R\bar{3}$

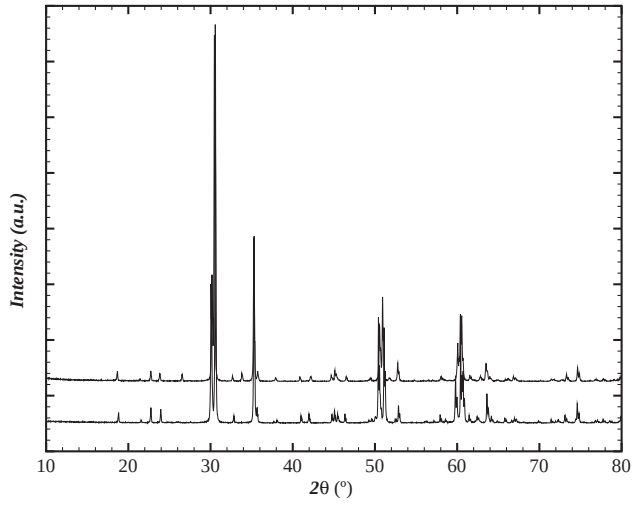

Fig. 1. XRPD patterns (Cu$K\alpha$) of $In_{5.5}Sb_{1.5}O_{12}$ (down) and $In_4Sn_3O_{12}$ (up).

with two sets of cationic positions 3(*a*), 18(*f*) and three sets of oxygen positions 18(*f*), in the corresponding hexagonal cell ($a \sharp 9.5$ Å and $c \sharp 8.9$ Å). For the different compositions, the convergence of the refinements was easily obtained, resulting in satisfying values of the confidence factors (Table 1). The calculated patterns fit with the experimental one, as shown for the limit compound $In_{5.5}Sb_{1.5}O_{12}$ (Fig. 2). As exemplified for $In_{5.5}Sb_{1.5}O_{12}$, the atomic coordinates (Table 2) show that the cationic positions of these phases are very close to those previously observed for $In_4Sn_3O_{12}$ [16], whereas in contrast, the oxygen positions are significantly shifted with respect to those of $In_4Sn_3O_{12}$, even if we bear in mind that the accuracy of the latter obtained here by XRPD, is lower than that obtained by neutron powder diffraction for $In_4Sn_3O_{12}$ [16]. It is, of course, not possible to distinguish the Sb from the In or Sn positions from XRPD structure calculations, due to the close atomic number of these elements, but the examination of the interatomic distances (Table 3) gives a clear answer to this question. The *M*–O distances in the 3(*a*) site (1.95 Å) are significantly smaller than those in the 18(*f*) site (2.04–2.60 Å) and than those observed for the 3(*a*) site in $In_4Sn_3O_{12}$. This shows that the 3(*a*) sites are preferentially occupied by antimony and that most probably for the limit phase $In_{5.5}Sb_{1.5}O_{12}$, the 3(*a*) sites are totally occupied by antimony, whereas the additional Sb is statistically distributed in the 18(*f*) sites with In, according to the formula $[In_{5.5}Sb_{0.5}]_{18(f)}[Sb]_{3(a)}O_{12}$. Such an ordered cationic distribution is greatly supported by the tendency of Sb^{5+} to accommodate a highly symmetrical octahedral coordination, as previously shown by one of us (J.C.) in the complex bixbyite $Cu_3TiFeSbO_9$ [18]. The smaller size of Sb^{5+} compared to In^{3+} and Sn^{4+}, according to Shannon and Prewitt [19], corroborates this view point. The evolution of the cell parameters versus *x* (Table 1 and Fig. 3) supports also strongly this ordered cationic distribution. One indeed observes that the "*a*" parameter exhibits a singular point at $x = 1$ (Fig. 3a), decreasing below $x = 1$, and increasing beyond this value, whereas the "*c*" parameter increases continuously with *x* (Fig. 3b), suggesting two regimes in the cationic distribution versus *x*, in agreement with the above observations. The rupture in the cell volume evolution versus *x*, at $x = 1$ (Fig. 3c) is also in agreement with this interpretation.

Electrical resistivity measurements were carried out by the four-probe method in the range 5–375 K, using a PPMS facility, on pellets sintered at 1400 °C in air. For these experimental conditions, three samples corresponding to compositions ($x = 0.50$, 0.66 and 1) were explored and for reference, a sample of $In_4Sn_3O_{12}$ sintered in the same conditions was also measured. For $x > 1$, the instability of the materials above 1300 °C did not allow any sintering to be achieved, so that no

Table 1
Crystal chemical data of the solid solution $In_{4+x}Sn_{3-2x}Sb_xO_{12}$ $0 \leqslant x \leqslant 1.5$

Comp. x	0	0.33	0.50	0.66	1.0	1.33	1.50
Temp. (°C)	1400	1400	1400	1400	1400	1250	1250
a (Å)	9.4637(2)	9.4564(2)	9.4537(2)	9.4529(2)	9.4478(2)	9.4521(1)	9.4545(1)
c (Å)	8.8554(2)	8.8740(2)	8.8810(2)	8.8888(2)	8.9034(2)	8.9191(1)	8.9210(2)
V (Å^3)	687.36	687.74	687.95	688.35	688.76	690.60	691.10
R_b	7.7	4.1	4.9	4.7	4.7	4.6	8.2
R_p	16.4	13.3	14.1	14.9	12.5	12.5	17.5

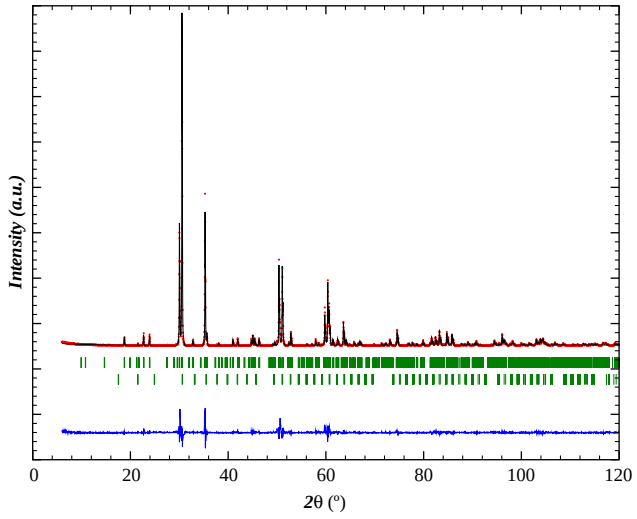

Fig. 2. Observed (dots), calculated (lines) and difference XRPD pattern of $In_{5.5}Sb_{1.5}O_{12}$. Vertical bars indicate the positions of the reflections of the title phase (upper) and In_2O_3 (lower). The calculated amount of the latter phase does not exceed 1%.

resistivity measurements were carried out. The $\rho(T)$ curves of the $In_{4+x}Sn_{3-2x}Sb_xO_{12}$ samples (Fig. 4) clearly show the decrease of the resistivity, due to the introduction of antimony. Starting from $In_4Sn_3O_{12}$ ($x = 0$), which exhibits at room temperature (RT) a resistivity of $2.6 \times 10^{-2}\,\Omega\,cm$ close to that previously observed ($2 \times 10^{-2}\,\Omega\,cm$) for a ceramic sample by several authors [13,20], there is a first step for both compositions $x = 0.50$ and 0.66: $\rho_{RT} \sharp 10^{-2}\,\Omega\,cm$. A further decrease occurs for $x = 1$, i.e., In_5SnSbO_{12} which clearly shows the best performances ρ_{RT}: $2.8 \times 10^{-3}\,\Omega\,cm$. Thus, the resistivity of the new oxide In_5SnSbO_{12} is one order of magnitude smaller than that of $In_4Sn_3O_{12}$ and less than one order of magnitude larger than that of the well-known ITO: approximately $0.5 \times 10^{-3}\,\Omega\,cm$ for a 3% Sn ceramic fired at 1400 °C in air [21]. Moreover, the temperature dependence of In_5SnSbO_{12} is practically semi-metallic instead of semi-conductive for $In_4Sn_3O_{12}$.

The optical properties of these oxides show their potential as transparent conductors. The color of the samples ranges from pale yellow ($x = 0$) to light green ($x = 1$). Diffuse reflectance spectra (Fig. 5) registered for $x = 0.50$; 0.66 and 1, with a double beam spectrophotometer (Cary Varian), are very similar to that of $In_4Sn_3O_{12}$. One indeed observes that up to $x = 1$, the introduction of antimony decreases only slightly the maximum percent reflectance around 500 nm, with

Table 2
Atomic parameters of $In_{5.5}Sb_{1.5}O_{12}$—XRPD Rietveld refinement—and $In_4Sn_3O_{12}$—NPD Rietveld refinement [16]

Formula	$In_{5.5}Sb_{1.5}O_{12}$		$In_4Sn_3O_{12}$	
Cationic site 3(a) 100% Sb or Sn[a]	B[b]	0.26 (9)	B[b]	0.54 (6)
Cationic site 18(f)	x	0.2518 (2)	x	0.2526 (2)
8.33% Sb or 33% Sn	y	0.2143 (2)	y	0.2145 (2)
91.66% In or 67% In	z	0.3497 (2)	z	0.3497 (2)
	B[b]	0.28 (4)	B[b]	0.47 (4)
O_1 site 18(f)	x	0.1920 (17)	x	0.1979 (2)
	y	0.1653 (27)	y	0.1768 (2)
	z	0.1073 (15)	z	0.1162 (2)
	B[b]	2.4 (5)	B[b]	0.96 (4)
O_2 site 18(f)	x	0.1921 (23)	x	0.1886 (3)
	y	0.9775 (23)	y	0.9745 (2)
	z	0.3830 (14)	z	0.3917 (2)
	B[b]	1.8 (4)	B[b]	0.82 (3)

[a] $x, y, z = 0$.
[b] Isotropic thermal factor in Å^2.

Table 3
Metal–oxygen distances (Å) in $In_{5.5}Sb_{1.5}O_{12}$ and $In_4Sn_3O_{12}$ [16]

Formula	$In_{5.5}Sb_{1.5}O_{12}$		$In_4Sn_3O_{12}$	
M–O in 3(a)	M–$O_1 \times 6$	1.95 (2)	M–$O_1 \times 6$	2.057(2)
M = Sb or Sn				
	M–$O_1 \times 1$	2.22 (3)	M–$O_1 \times 1$	2.118(3)
	M–$O_1 \times 1$	2.21 (3)	M–$O_1 \times 1$	2.145(3)
M–O in 18(f)	M–$O_1 \times 1$	2.60 (3)	M–$O_1 \times 1$	2.643(3)
$M = (In_{0.92}Sb_{0.08})$	M–$O_2 \times 1$	2.04 (3)	M–$O_2 \times 1$	2.070(3)
$M = (In_{0.67}Sn_{0.33})$	M–$O_2 \times 1$	2.11 (3)	M–$O_2 \times 1$	2.146(3)
	M–$O_2 \times 1$	2.19 (3)	M–$O_2 \times 1$	2.178(3)
	M–$O_2 \times 1$	2.40 (3)	M–$O_2 \times 1$	2.313(3)
	Average 2.25		Average 2.230	

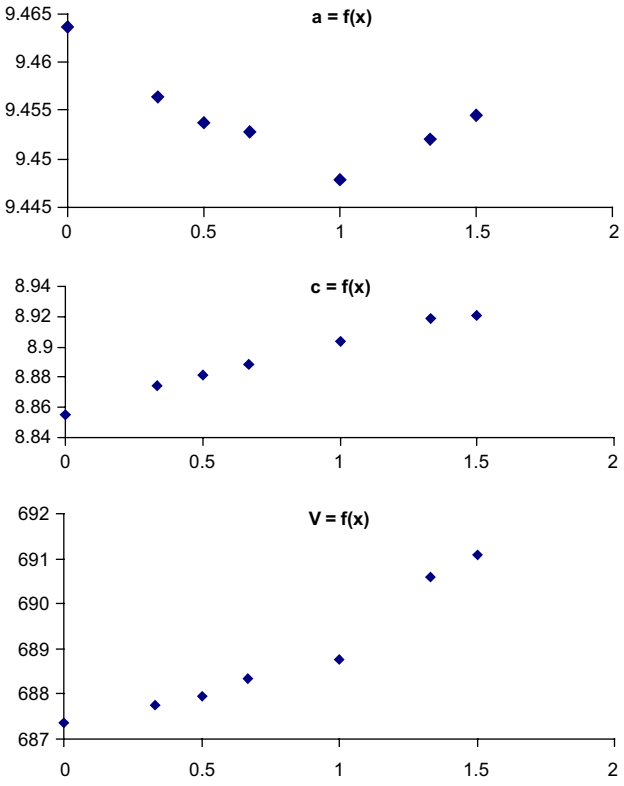

Fig. 3. Variation of the hexagonal cell constants in the solid solution $In_{4+x}Sn_{3-2x}Sb_xO_{12}$.

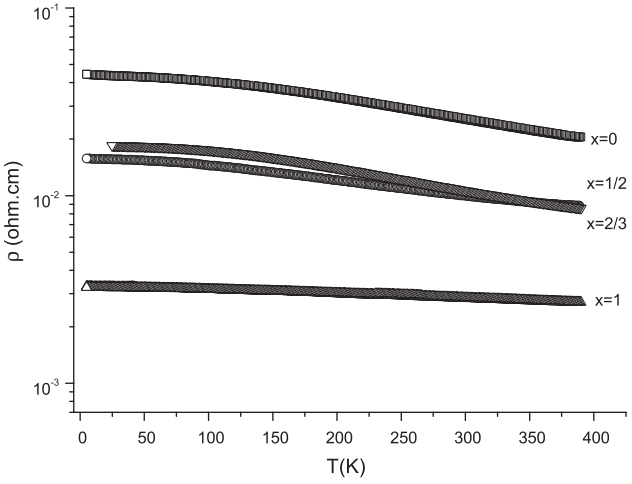

Fig. 4. Electrical resistivity (Ω cm) versus temperature (K) in the solid solution $In_{4+x}Sn_{3-2x}Sb_xO_{12}$.

respect to $In_4Sn_3O_{12}$. Simultaneously, a small increase of the optical bandgap, by about 0.15 eV, occurs.

In conclusion, this study shows the great potential of pentavalent antimony to increase the conductivity in the ordered oxygen-deficient fluorite oxides $In_{4+x}Sn_{3-2x}Sb_xO_{12}$. The properties of these new transparent conductors are most probably closely related to the d^{10} electronic configuration of Sb(V) which may contribute to the position of the conduction band. The mechanism

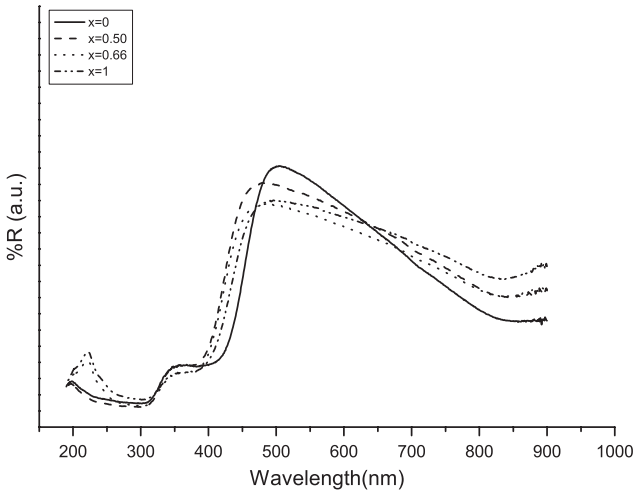

Fig. 5. Measured optical reflectance in the solid solution $In_{4+x}Sn_{3-2x}Sb_xO_{12}$.

of the conductivity is still a matter of debate, and it is possible that the ordering of the Sb^{5+} and In^{3+}/Sn^{4+} species over the 3(a) and 18(f) sites, respectively, plays an important role in such properties. Further investigations of pentavalent antimony-based oxides should allow new TCOs to be discovered.

References

[1] H.L. Hartnagel, A.L. Dawar, A.K. Jain, C. Jagdish, Semi-Conducting Transparent Thin Films, IOP publishing, Bristol and Philadelphia, 1995.
[2] D.S. Ginley, C. Bright, MRS Bull. 8 (2000) 15.
[3] B.G. Lewis, D.C. Paine, MRS Bull. 8 (2000) 22.
[4] T. Minami, MRS Bull. 8 (2000) 38.
[5] A.J. Freeman, K.R. Poeppelmeier, T.O. Mason, R.P.H. Chang, T.J. Marks, MRS Bull. 8 (2000) 45.
[6] H. Kawazoe, H. Yanagi, K. Ueda, H. Hosono, MRS Bull. 8 (2000) 28.
[7] J.C.C. Phan, F.J. Bachner, J. Electrochem. Soc. 122 (1975) 1719.
[8] W.G. Haines, R.H. Bube, J. Appl. Phys. 49 (1978) 223.
[9] G. Frank, H. Köstlin, Appl. Phys. Solids Surf. 27 (1982) 197.
[10] M. Mizuhashi, Thin Solid Films 70 (1980) 11.
[11] R.B.H. Tahar, T. Ban, Y. Ohya, Y. Takahashi, J. Appl. Phys. 83 (1998) 2631.
[12] H. Enoki, J. Echigoya, H. Suto, J. Mater. Sci. 13 (1975) 192.
[13] J.L. Bates, C.W. Griffin, D.D. Marchant, J.E. Garnier, Am. Ceram. Soc. Bull. 65 (1986) 673.
[14] H. Enoki, J. Echigoya, Phys. Stat. Sol. (a) 132 (1992) 151.
[15] T. Minami, Y. Takeda, S. Takata, T. Kakumumi, Thin Solid Films 308 (1997) 13.
[16] N. Nadaud, N. Lequeux, M. Nanot, J. Jové, T. Roisnel, J. Solid State Chem. 135 (1998) 140.
[17] J. Rodriguez-Carvajal, Program Fullprof 3 (1997) 5.
[18] J. Choisnet, P. Mouron, Mater. Res. Bull. 22 (1989) 1355.
[19] R.D. Shannon, C.T. Prewitt, Acta Crystallogr. B 25 (1969) 925.
[20] W. Pitschke, J. Werner, G. Behr, K. Koumoto, J. Solid State Chem. 153 (2000) 349.
[21] A. Ambrosini, A. Duarte, K.R. Poeppelmeier, M. Lane, C.N. Kannewurf, T.O. Mason, J. Solid State Chem. 153 (2000) 41.